

Research Article

DOI:10.13179/canchemtrans.2013.01.04.0039

Crystallization Kinetics of Isotactic Polystyrene from Molten and Glassy States

Al Mamun^{1*}, Norimasa Okui¹ and Mohammad A K Khan²¹Department of Organic and Polymeric Materials, International Polymer Research Center, Tokyo Institute of Technology, O-okayama, Meguro-ku, Tokyo, Japan²Department of Chemistry and Chemical Biology, McMaster University, Hamilton, Ontario, Canada L8S 4M1*Corresponding Author, Email: amamun@fsu.edu, Phone: +18504106296, Fax: +18504106296**Received:** September 12, 2013 **Revised:** October 11, 2013 **Accepted:** October 12, 2013 **Published:** October 13, 2013

Abstract: Crystallization rate of isotactic polystyrene (iPS) from molten and glassy state was studied by polarized optical microscopy (POM), differential scanning calorimetry (DSC) and light intensity measurement (LIM) techniques. Samples were melted at different temperatures and subsequently crystallized from molten or glassy states. In all cases, the crystallization rate shows a temperature dependent bell shaped curve. At low melting temperatures, the crystallization rate is faster, due to insufficient melting, where the surviving crystals accelerate the crystallization process. With the increasing melting temperatures, crystallization rate slows down. At high melting temperature, the crystallization rate from glassy state is faster than from the molten state. The crystallization rates from molten states strongly depend on the crystallization temperatures and melting temperatures, where it depends only on crystallization temperatures in case of glassy states. These crystallization rates are discussed using Avrami equation.

Keywords: Crystallization Rate, Avrami Equation, Melt Temperature, Isotactic Polystyrene

1. INTRODUCTION

The overall crystallization rate of a semi-crystalline polymer is mainly governed by the primary nucleation and the crystal growth rate [1]. Primary nucleation is the formation of a new three-dimensional solid phase from the melt phase. Primary nuclei can be formed at random sites in the melt (homogeneous nucleation) or on a foreign body such as an impurity particle or a polymerization catalyst acting as a nucleation center (heterogeneous nucleation). When impurities or residual crystals are present, the nucleation rate depends on the thermal history of the polymer and, more specifically, on the previous melting temperature, until a temperature is reached where all possible sources for nucleation are destroyed. After the nucleus is formed, a new layer grows by secondary nucleation, a process similar to primary nucleation known as growth rate. This rate can be determined directly by optical or electron

microscopy or, indirectly, by the increase in the crystalline content. In case of direct measurement, the spherulites are assumed to be initiated from primary nuclei. The nucleation rate is measured by the number of nuclei with time per unit volume. The growth rates are measured by the radial growth with time observed by POM. So the spherulites are the main morphological form of polymers crystallized from molten and glassy states. The study of the kinetics of this phase transformation is of primary importance for technological profit, as the crystallization mechanism controls the spherulitic texture, which in turn affects the mechanical properties like impact strength, a great parameter of future industrial application. However, the overall crystallization rate and the nucleation and growth rate depend strongly on crystallization temperature (T_c). Depending on the initial state, the crystallization process can be classified into two categories—(i) melt-crystallization, where the initial state is melt and the polymer samples should stay in the molten state for a sufficient time before being crystallized and (ii) glass-crystallization, where the initial state is a glassy state, a temperature lower than its T_g , before crystallization.

Isotactic polystyrene is a good polymer for its higher glass transition temperature, can be rapidly transfer to glassy state without crystallization. This is important for industrial applications like packaging, building construction, and in injection molding applications and especially for film and sheet where the solidification of molten polymer is governed by crystallization rate. Several reports have appeared in the literature on the melt crystallization of iPS [2-6]. Boon *et al.* have studied the crystallization kinetics of melt crystallized isotactic polystyrene by dilatometry [2-3]. The authors reported two nucleation mechanisms for resistance and induced nuclei. The number of induced nuclei is decreased by purifying the polymer and by the heating above the melt temperature. Only the resistant nuclei remain above the melting temperature. They also found, the slowness of crystallization of iPS is mainly a consequence of the lower mobility of the molecules caused by the bulky phenyl group. Jianming *et al.* investigated the isothermal crystallization process of iPS from melt and glassy state by IR and found different bands for the cold- and melt-crystallization processes [4]. The morphology of quiescent and shear-induced isothermal crystallization of isotactic polypropylene (iPP) was studied by Phillips A. and found that during isothermal crystallization the shear-induced nuclei promote oriented α form crystal growth, accelerate the crystallization kinetics and ultimately swamp the effect of the nucleating particles present [7]. In our previous study, we reported the influence of thermal history on the nucleation rate and crystal growth rate for iPS [8-9].

In this paper, we report the overall crystallization rate using Avrami equation for iPS both from molten and glassy states since Avrami equation is the most common method to describe the isothermal crystallization process of polymers [10], copolymers [11] and blends [12-13]. To the best of our knowledge, this is the first report of overall crystallization rate for iPS using Avrami equation by LIM technique.

2. EXPERIMENTAL

Sample of iPS ($M_w=17,800$, $M_n=10,600$, $M_w/M_n=1.68$, Tacticity: 96%) was supplied by Idemitsu Kosan Co., Ltd. The sample was melted between two cover glasses using a metallic spacer to form a given film thickness on a hot stage. The sample was melted for five minutes at a temperature below and above the equilibrium melting temperature of 242°C (T_m^0) [14]. DSC melting peak showed at about 224°C and the end of the melting curve (tail of the peak) at 228°C for iPS crystallized at 200°C for eight hours [9]. Therefore, several typical melt temperatures were selected between 225 and 250°C. Subsequently, the molten sample was cooled to a temperature with a cooling rate of 30°C/min (crystallization from molten state). In another experiment, the molten sample was rapidly quenched to below the glass transition

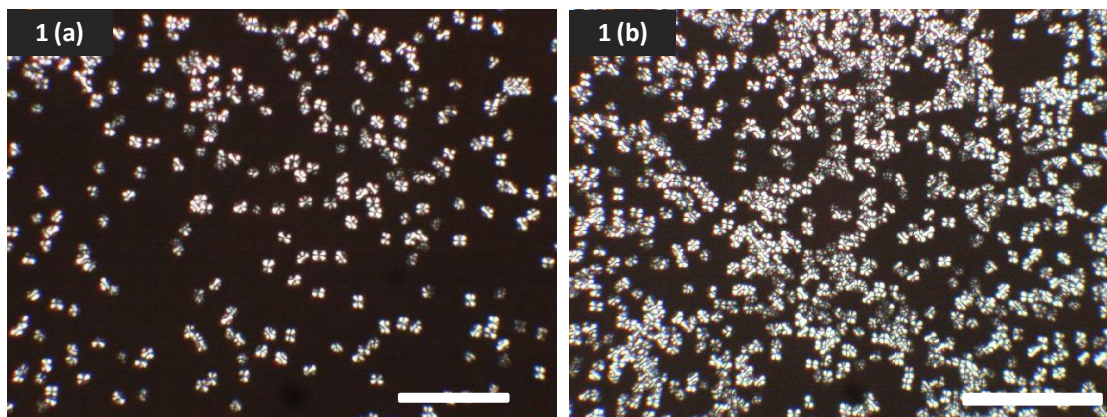


Figure 1: POM images for iPS crystallized at 160°C; a) molten state, and b) glassy state after melt from 230°C. The scale bar represents 100 μm .

temperature (90°C), hold for five minutes and then re-heated with 90°C/min to a crystallization temperature (crystallization from the glassy state).

2.1 Polarized Optical Microscopic (POM)

Polarized optical microscopy (POM) is contrast-enhancing technique that improves the quality of the image obtained with birefringence materials with polarized light. If both the analyzer and polarizer are crossed to each other, no light passing through the system and a dark viewfield present in the eyepieces. Depending on birefringence of the sample where the polarized light interacts strongly with the sample and generating contrast with the background. A Olympus BH-2 polarized optical microscope (POM) was used to capture images of the melt press films placed in a Linkam hotstage, including a temperature controller and a cooling unit. Photomicrographs were recorded with a CCD camera, Pixel 600ES. The saturated nucleation density is calculated by counting the number of small spherulites per unit volume of the sample observed by POM.

2.2 Differential Scanning Calorimetry (DSC)

The isothermal crystallization studies were carried out by a TA-60 DSC calorimeter. All the measurements were taken under nitrogen atmosphere to minimize the oxidative degradation. Films, about 150 μm thick, were prepared from the original powders by melting between Teflon foil in a Carver press at 250°C under low pressure and quenching at room temperature. To ensure good contact, a single flat piece, ~ 5 mg, was cut from each sample and placed in DSC aluminum pans. The instruments were calibrated with Indium, and the calibration checked every day.

2.3 Light Intensity Measurements (LIM)

Light intensity measurements were performed by the same temperature controller and optical microscope (OM) with a special filter of 550 nm and using Lux meter of LX-1330. The CCD camera attached to the microscope and connected to a computer permitted image acquisition; the crystallization process was recorded with time by means of software till complete crystallization (verified by direct OM observation). The intensity of these images was measured using software made in our laboratory and converted to equivalent Lux value with calibration curve. The light intensity data are found identical with the conventional DSC data (see supporting information). The relative crystallinity was calculated by normalizing the intensity of the fully crystallized image. The whole procedure was performed *in-situ*

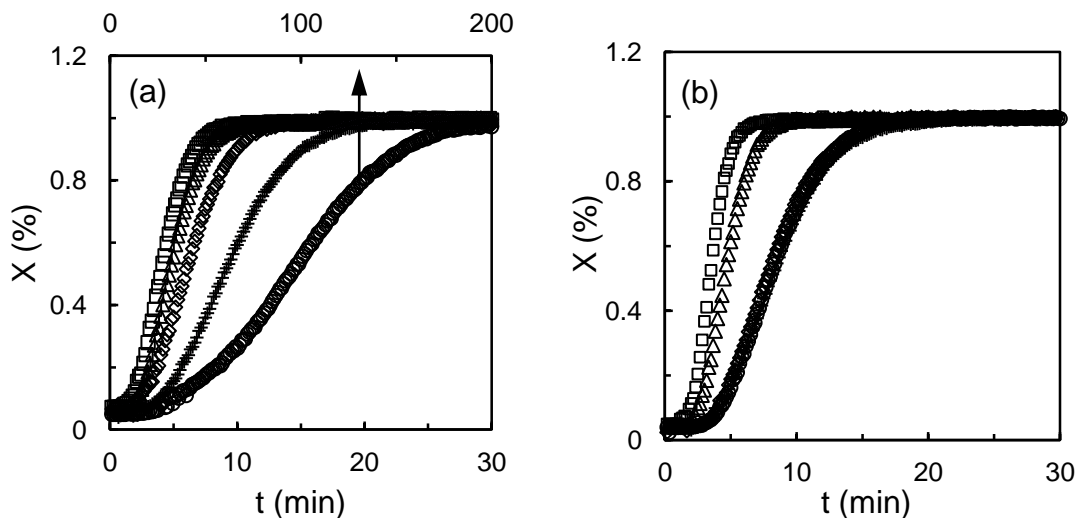


Figure 2: Plots of relative crystallinity versus crystallization time at 160°C as a function of melt temperature: a) from molten state of 228 (□), 230 (Δ), 232 (◇), 234 (+), 250 (○) and, b) glassy state of 228 (■), 230 (▲), 235 (◆), 240 (+), 250°C (●).

without moving the sample from the hot stage.

3. RESULTS AND DISCUSSION

Images of iPS crystallized at 160°C from molten and glassy state were studied using POM. Figure 1 shows a well-developed spherulitic morphology from both molten and glassy states. The number of spherulites is higher for glassy state, makes higher crystallinity in contrast with molten state. During melting of the polymer, the light cannot pass through the system and the background shows dark. After an initial induction time the spherulites start to developed, light can scatter from the developed crystals, pass through system, and the intensity as well as the degree of crystallinity increases with time. The well-known Avrami equation is often used to analyze the crystallization kinetics, assuming that the relative degree of crystallinity develop with time is [15-16]

$$X = 1 - \exp(-k t^n) \quad (1)$$

Where X is the degree of crystallinity, t is the crystallization time, k is the crystallization rate constant, and the exponent n represents the nucleation mechanism and growth dimensions. The value of n can be any positive integer between 1 and 4 [14]. In many polymers, the melt temperature does not influence the subsequent crystallization rate. Crystallization rate was found to be constant when the melting point exceed by as little as 0.1°C and to remain so for at least a further 70°C [17]. For i-PS the crystallization behavior was found different when the melting point exceed. Figure 2 shows the relative crystallinity of iPS with time crystallized at 160°C from molten state and glassy state. As can be seen, all the curves have a sigmoidal shape and the crystallinity increases with an initial induction time, increases with steady state, and then reach to a maximum value, a typical behavior of polymer crystallization. From molten states, the time (t_{max}) required to reach the maximum crystallinity is found to be dependent on melt temperature. The time is shorter when crystallized from lower melt temperature and become longer with higher melt temperature. For example, only seven minutes is needed to reach its maximum crystallinity after melt

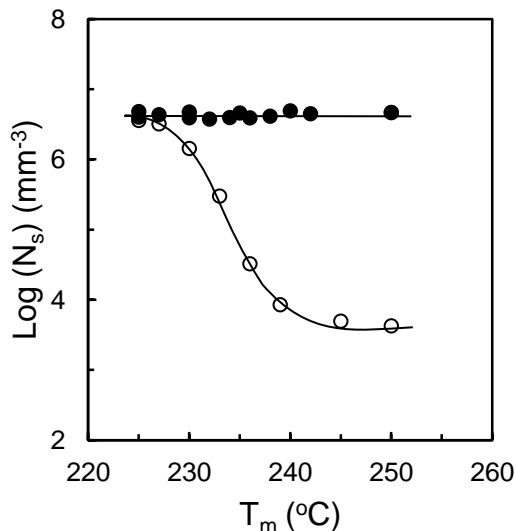
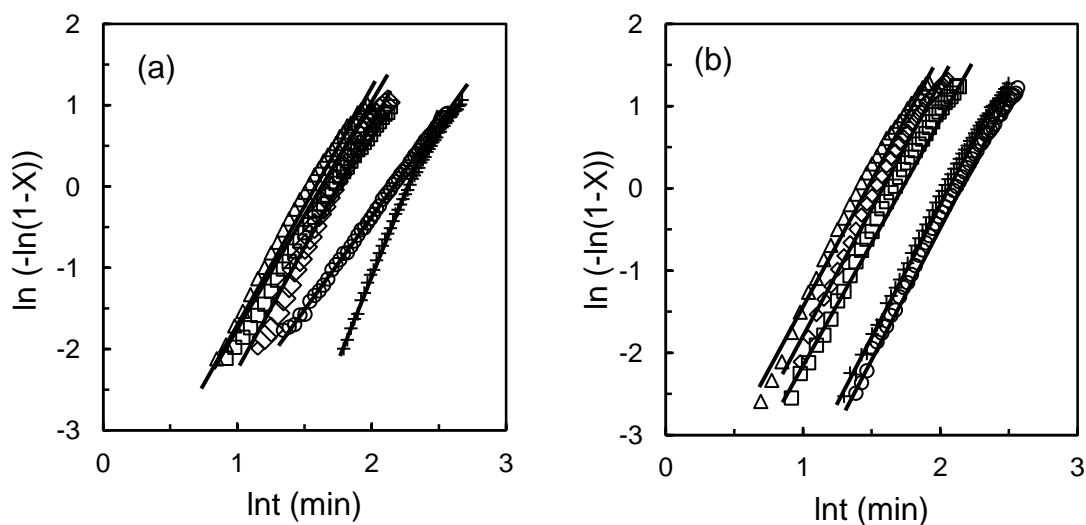


Figure 3: Melt temperature, T_m , dependence of saturated nucleation density, N_s from melt state (open symbol) and, from glassy state (solid symbol).

from 228°C, where it takes three hours from melt of 250°C (Fig.2a). On the other hand, no significant change in time was found from all glassy states, except at much lower melt temperature (Fig. 2b). This behavior can be related to melt temperature dependence saturated nucleation density N_s , where N_s is defined as the density of the limited number of effective sites for the nucleation process, or as a density of the surviving crystal nuclei in the polymer melt, which might be the center of spherulite. When the spherulites are not melted completely, the scaffold of the crystals remains in the polymer melts and can act as a nucleation center that increases nucleation density significantly. Figure 3 shows a common logarithm of the saturation nucleus density as a function of the melt temperatures for both molten and glassy state. The nucleation density is measured by counting number of spherulites captured by POM per unit volume. It should be noted that in all experiments the samples are crystallized from different melt temperatures, but always crystallized at same temperature ($T_c=160^\circ\text{C}$). The saturated nucleus density is found very high when crystallized from melt below 230°C due to insufficient melting of crystal which keep the heterogeneous system. Above 230°C, the saturation density rapidly decreases within the temperature range of 230–245°C as the induced nuclei is destroyed by increased temperature, and it tends to more homogeneous melt. At higher temperature (for example 250°C), this density levels off to a constant value due to some heterogeneities may survive in polymer melt at temperature higher than the melting point. The saturation densities below 230°C are found three orders of magnitude higher than those above 250°C. These results indicate that the heterogeneities decrease rapidly with an increase in the melt temperature and it is almost disappear at higher melt temperatures. The corresponding t_{max} values vary simultaneously. From glassy state, the saturation nucleus densities remain identical with melt temperatures. This may be due to the same density fluctuation for enthalpy relaxation, where the crystallization process started from a unique phase (same glass temperature and holding time) and always same number of induced nuclei is generated. The additional sites are caused by insufficient melting of the original spherulites below 230°C, which takes shorter time to reach maximum crystallinity as shown for melt at 228° and 230°C in Fig. 2. From this experiment, it is concluded that during crystallization from molten states, the nucleation density strongly depends on melt temperature, where it is independent from glassy states.

Table 1. Avrami exponent (n) calculated for iPS crystallized at various temperatures from the melt and glassy state based on the Eq. 1.

Crystallization temperature (°C)	Avrami exponent, n			
	Melt states		Glassy states	
	230°C	250°C	230°C	250°C
150	2.27	2.05	3.17	2.58
160	2.54	2.10	3.11	2.71
170	2.97	2.13	3.17	2.63
180	3.29	2.17	3.26	3.02
190	3.55	2.74	3.29	2.97

**Figure 4:** Avrami plots at various crystallization temperatures: a) from melt and, b) glassy states. Symbols are indicating as 150 (○), 160 (□), 170 (Δ), 180 (◇), and 190°C (+).

Using Eq. (1) in its double-logarithmic form, and plotting $\ln(-\ln(1-X))$ against $\ln t$, the Avrami exponent n and k are obtained from the slope and intercepts of the plot. Figure 4 shows a typical plot of $\ln(-\ln(1-X))$ with time as a function of crystallization temperatures from the melt and from the glassy state after melt from 230°C. It seems that the slopes and intercepts of the plots vary with T_c for molten state, but for glassy state the slopes remain almost constant while the intercepts change, indicating the similar values of n with different k . The values of Avrami exponent n calculated for various T_c from both the molten and the glassy states at two different melt temperatures are summarized in Table 1. It is noted that for the glassy states, the values are always close to 3. On the other hand, for the molten state, the n values are between 2.0 and 3.5 suggesting the crystallization corresponds to spherical diffusion control growth with thermal nucleation [18].

Figure 5 shows the temperature dependence of the crystallization rates as calculated using Eq. (1) from molten and glassy state at different melt temperatures. The temperature dependence of crystallization rate shows bell shape dependence, with a maximum rate for both molten and glassy states. The crystallization rate at 160°C from molten state decreases with melt temperatures, where the rate

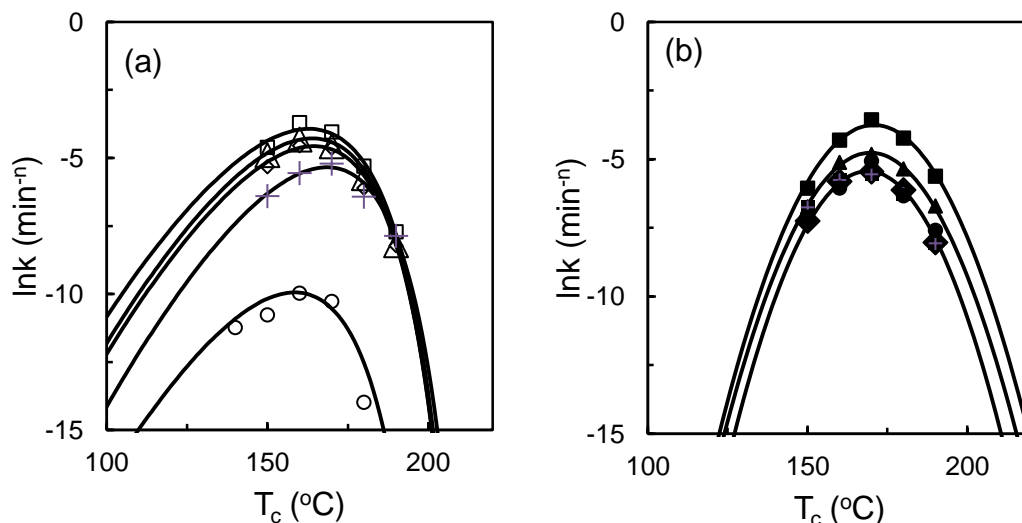


Figure 5: Crystallization temperature, T_c , dependence of crystallization rate, lnk , as a function of melts temperature. Symbols are indicating as shown in Figure 2.

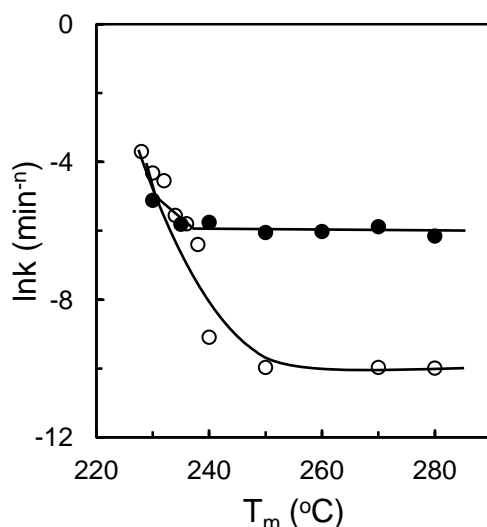


Figure 6: Melt temperature, T_m , dependence of crystallization rate, lnk , from melt state (open symbol) and, from glassy state (solid symbol).

remains same from glassy states (Fig. 5b). Similar temperature dependence behavior for primary nucleation rate and crystal growth rate of this polymer is reported earlier in our investigations [8-9]. However, at this stage, it is difficult to clarify whether the primary nucleation rate or crystal growth rate or both are dominant in the overall crystallization rate.

The melt temperature dependence of the crystallization rate constant where the samples were melted at different melt temperatures (225-250°C) and crystallized at same temperature (160°C) from both molten and glassy state is shown in figure 6. Below 230°C, the crystallization rate is found to be very fast. Above 230°C, the rate decreases rapidly within a temperature range of 230-240°C and levels off to a constant value. The rate constant at temperatures below 230°C is few orders of magnitudes higher than

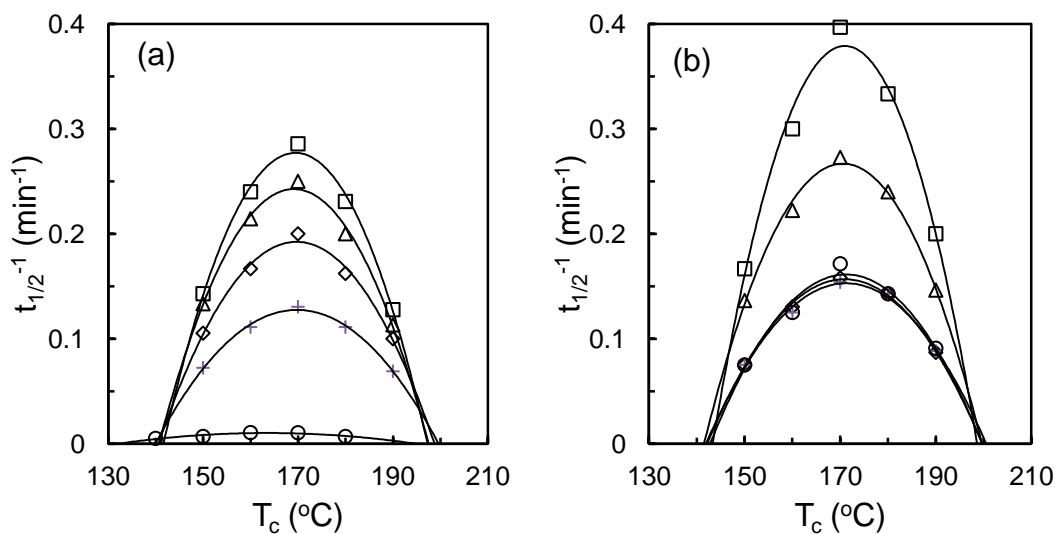


Figure 7: Crystallization temperature, T_c , dependence of half-time, $t_{1/2}^{-1}$, as a function of melts temperature; a) from melt and, b) from glassy state. Symbols are indicating as shown in Figure 2.

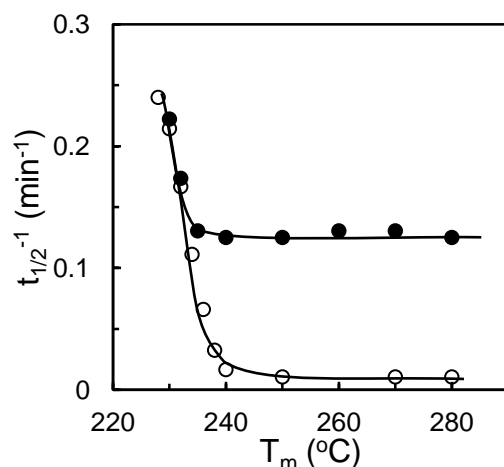


Figure 8: Melt temperature, T_m , dependence half-time, $t_{1/2}^{-1}$, from melt state (open symbol) and from glassy state (solid symbol).

those at temperatures above 250°C. This is due to the results of melt temperature dependence number of saturated nucleus density that discussed earlier. This suggests that in case of molten state, the crystallization temperature dependent rate depends on the melt temperature but in case of glassy states it is independent of melt temperature.

The half-time for full crystallization $t_{1/2}$, is the time required to achieve 50% of the final crystallinity of the samples, is an important parameter for the discussion of crystallization kinetics. Usually, the crystallization rate is described as the reciprocal of $t_{1/2}$, namely $t_{1/2}^{-1}$. The value of $t_{1/2}$ was calculated by the following equation based on Eq. 1 as:

$$t_{1/2} = \left(\frac{\ln 2}{k} \right)^{1/n} \quad (2)$$

Figure 7 shows the crystallization temperature dependence of $t_{1/2}^{-1}$ crystallized a) from melt and, b) from glassy state. It is found that the $t_{1/2}^{-1}$ increases with temperature until reaches a maximum and then decreases, also showing a bell shaped dependence. The $t_{1/2}^{-1}$ values always show a maximum at same temperature at $\sim 170^\circ\text{C}$. The growth rate also showed bell shaped temperature dependence with a maximum at the same temperature, indicate that the slower growth rate takes longer time and relatively faster growth rate takes shorter time to reach the maximum crystallinity.

The change of the half-time for full crystallization with melt temperature was also observed. Figure 8 shows $t_{1/2}^{-1}$ as a function of melt temperature from both molten and glassy state. As for the molten state, the $t_{1/2}^{-1}$ values are very high below 230°C and remain constant. However, above 230°C , the $t_{1/2}^{-1}$ decreases rapidly within a temperature range of $230\text{--}240^\circ\text{C}$ and levels off to a constant value. The $t_{1/2}^{-1}$ values at temperatures above 250°C are 20 times lower than those at temperatures below 230°C . On the other hand, the $t_{1/2}^{-1}$ values of crystallization from glassy state remain almost the same at above 230°C . This behavior is the reflection of the melt temperature depended crystallization rate that is based on melt temperature depended nucleation densities.

From the above observations we can summarized that above the melting temperature ($228\text{--}230^\circ\text{C}$) there are many nucleation sites in iPS, and the crystallization rate is very fast and takes short time for complete crystallization. At 230°C , the spherulites are melted but their structures are not completely destroyed as can be seen from the tail of DSC melting curve showed at 228°C . Above 230°C , the nucleation density decreases rapidly within a temperature range of $230\text{--}240^\circ\text{C}$ and levels off to a constant value. Consequently, the crystallization rate becomes slower and the relative crystallization time takes longer for complete crystallization. When the sample is melt far above the melting temperature (e.g., 250°C) all induced nuclei disappear, only the pre-existing nuclei remains but the order of the density is very low in comparison to one below 230°C . As a result the crystallization rate become very slow and takes longer time for completion. On the other hand, in case of crystallization from the glassy state, induced nuclei are always generated due to the same enthalpy relaxation, a unique state, that has the same in number of nuclei, shows always the same crystallization rate and time for complete crystallization.

4. CONCLUSIONS

The isothermal crystallization behavior of iPS from molten and glassy states was studied. The crystallization rates are fast both from melt and glassy states at lower temperatures due to insufficient melting of the spherulites. The crystallization rate decreases with melt temperature due to decrease of the saturated nucleation density. The crystallization rate from glassy state is always faster than that from molten states. Both the crystallization rate and crystallization half-time shows bell shape temperature dependence. Crystallization from molten states depends on the crystallization rate constant and half-time depends on crystallization temperature, melt temperature and saturated nucleation densities. On the other hand, crystallization from glassy state depends only on crystallization temperature, and is independent of melt temperature and saturated nucleation densities. Crystal nucleation or growth rate or both might be the dominant part for the overall crystallization kinetics, and the conformation that remains even higher melt temperatures are the future issue and will be published elsewhere.

SUPPORTING INFORMATION

Figure S1, S2 and S3 are included in the supporting information. This document is available at http://canchemtrans.ca/uploads/files/Supporting_Information_0039.pdf

ACKNOWLEDGMENT

The authors are grateful to Professor Gert Strobl, University of Freiburg, Germany, for his helpful discussions. The authors are also grateful to Ministry of Science and Education, Japan for financial support.

REFERENCES AND NOTES

- [1] Mandelkern, L., *Crystallization of Polymers*. McGraw-Hill, Inc: New York, 1964.
- [2] Boon, J.; Challa, G.; Van Krevelen, D. W., Crystallization kinetics of isotactic polystyrene. I. Spherulitic growth rate. *J. Polym. Sci. Part A-2: Polym. Phys.* **1968**, *6(10)*, 1791-1801.
- [3] Boon, J.; Challa, G.; van Krevelen, D. W., Crystallization kinetics of isotactic polystyrene. II. Influence of thermal history on number of nuclei. *J. Polym. Sci. Part A-2: Polym. Phys.* **1968**, *6(11)*, 1835-1851.
- [4] Zhang, J.; Duan, Y.; Sato, H.; Shen, D.; Yan, S.; Noda, I.; Ozaki, Y., Initial Crystallization Mechanism of Isotactic Polystyrene from Different States. *J. Phys. Chem. B* **2005**, *109(12)*, 5586-5591.
- [5] Imanari, K.; Yota, S.; Hashimoto, M.; Fujiwara S.; Itoh, T. *Polym. Preprints* **2005**, *54*.
- [6] Taguchi, K.; Miyaji, H.; Izumi, K.; Hoshino, A.; Miyamoto, Y.; Kokawa, R., Growth shape of isotactic polystyrene crystals in thin films. *Polym.* **2001**, *42(17)*, 7443-7447.
- [7] Phillips, A.; Zhu, P.-W.; Edward, G., Polystyrene as a versatile nucleating agent for polypropylene. *Polymer* **2010**, *51(7)*, 1599-1607.
- [8] Mamun, A.; Umemoto, S.; Ishihara, N.; Okui, N., Influence of thermal history on primary nucleation and crystal growth rates of isotactic polystyrene. *Polym.* **2006**, *47(15)*, 5531-5537.
- [9] Mamun, A.; Umemoto, S.; Okui, N.; Ishihara, N., Self-Seeding Effect on Primary Nucleation of Isotactic Polystyrene. *Macromolecules* **2007**, *40(17)*, 6296-6303.
- [10] Kim, I. T.; Lee, J. H.; Shofner, M. L.; Jacob, K.; Tannenbaum, R., Crystallization kinetics and anisotropic properties of polyethylene oxide/magnetic carbon nanotubes composite films. *Polym.* **2012**, *53(12)*, 2402-2411.
- [11] Chiari, Y. L.; Vadlamudi, M.; Chella, R.; Jeon, K.; Alamo, R. G., Overall crystallization kinetics of polymorphic propylene-ethylene random copolymers: A two-stage parallel model of Avrami kinetics. *Polym.* **2007**, *48(11)*, 3170-3182.
- [12] Song, P.; Chen, G.; Wei, Z.; Chang, Y.; Zhang, W.; Liang, J., Rapid crystallization of poly(l-lactic acid) induced by a nanoscaled zinc citrate complex as nucleating agent. *Polym.* **2012**, *53(19)*, 4300-4309.
- [13] Takeshita, H.; Shiomi, T.; Takenaka, K.; Arai, F., Crystallization and higher-order structure of multicomponent polymeric systems. *Polym.* **2013**, *54(18)*, 4776-4789.
- [14] Hoffman, J. D., Davis, G.T., Lauritzen, J. I., Jr., *Treaties on Solid State Chemistry*. Plenum Press: New York, 1976.
- [15] Avrami, M., Kinetics of Phase Change. I General Theory. *J. Chem. Phys.* **1939**, *7(12)*, 1103-1112.
- [16] Avrami, M., Kinetics of Phase Change. II Transformation-Time Relations for Random Distribution of Nuclei. *J. Chem. Phys.* **1940**, *8(2)*, 212-224.
- [17] Banks, W.; Sharples, A., The effect of melt temperature on nucleation in crystallizing polymers. *Die Makromolekulare Chemie* **1963**, *67(1)*, 42-48.
- [18] Turnbull, D.; Fisher, J. C., Rate of Nucleation in Condensed Systems. *J. Chem. Phys.* **1949**, *17(1)*, 71-73.

The authors declare no conflict of interest

© 2013 By the Authors; Licensee Borderless Science Publishing, Canada. This is an open access article distributed under the terms and conditions of the Creative Commons Attribution license <http://creativecommons.org/licenses/by/3.0/>